AIP | Applied Physics Letters

Silver oxide Schottky contacts on n-type ZnO

M. W. Allen, S. M. Durbin, and J. B. Metson

Citation: Appl. Phys. Lett. **91**, 053512 (2007); doi: 10.1063/1.2768028
View online: http://dx.doi.org/10.1063/1.2768028
View Table of Contents: http://apl.aip.org/resource/1/APPLAB/v91/i5
Published by the American Institute of Physics.

Silver oxide Schottky contacts on *n*-type ZnO

M. W. Allen[a] and S. M. Durbin
Department of Electrical and Computer Engineering, University of Canterbury, Christchurch 8043, New Zealand

J. B. Metson
Department of Chemistry, University of Auckland, Auckland 1142, New Zealand

(Received 13 June 2007; accepted 10 July 2007; published online 3 August 2007)

A method of fabricating highly rectifying Schottky contacts on *n*-type ZnO using silver oxide has been developed and used to compare diode performance on hydrothermal and melt grown, bulk, single crystals. Silver oxide diodes on hydrothermal ZnO have lower ideality factors, lower reverse current voltage dependence, higher series resistance, and larger surface-polarity related differences in barrier height, compared to those on melt ZnO. These effects are explained by the large difference in resistivity between hydrothermal and melt ZnO. Barrier heights of 1.20 eV were achieved on the Zn-polar face of hydrothermal ZnO which are the highest reported for *n*-type ZnO. © *2007 American Institute of Physics*. [DOI: 10.1063/1.2768028]

In recent years, ZnO has been the subject of renewed interest with the aim of fabricating light detecting and emitting devices in the UV spectrum. The production of high quality *p-n* junctions has proved elusive because of difficulties in the growth of *p*-type material.[1] However, the fabrication of Schottky contacts on *n*-type ZnO allows the realization of a range of useful devices such as UV photodiodes, power diodes, and transistors.

The main "figures of merit" for Schottky contact performance are the effective barrier height (Φ_B) and the ideality factor (n). Figure 1 shows these parameters for the "best" Schottky contacts reported in the literature.[2–12] Values of n greater than unity are caused by nonideal behavior which includes image force lowering, thermionic field emission, and lateral contact inhomogeneity.[13] Among these, contact inhomogeneity is a dominant cause of high n values (>1.1) on reasonable quality, undoped material. A number of different surface pretreatments have been reported including the use of oxygen plasmas,[3,12] ozone,[9] and hydrogen peroxide.[10] However, the best reported Au and Pt Schottky contacts have been achieved on bulk ZnO wafers using just a simple surface clean with organic solvents.[4,11] This suggests that ZnO material quality, handling protocols, and contact deposition conditions may be more important factors. A number of researchers have reported significant age related improvements in Au, Ag, and Pd Schottky contacts,[4,14] which suggests that chemical bonding at the ZnO-metal interface may also be important.

In this letter, we report on the use of silver oxide to produce high quality rectifying contacts on *n*-type ZnO. Bulk grown, single crystal ZnO substrates were used: (1) a double sided polished, hydrothermally grown,[15] *c*-axis wafer (HT-1) from Tokyo Denpa Co. Ltd. was cut to provide Zn-polar and O-polar samples; (2) three single sided polished, pressurized melt grown,[16] wafers (PM-1, PM-2, and PM-3) from Cermet Inc. provided Zn-polar, O-polar, and *a*-plane samples, respectively. Table I gives the room temperature (RT) electrical characteristics of these bulk ZnO wafers obtained from Hall effect measurements using the van der Pauw geometry. The carrier concentration of "hydrothermal ZnO" is typically two to three orders of magnitude lower than that of "melt ZnO." This is mainly due to the presence of compensating Li and Na acceptor impurities in the hydrothermal material.[1,15]

Each as-received wafer was ultrasonically precleaned for 5 min in warm acetone followed by rinsing in methanol, isopropyl alchohol, and drying in N_2. The wafers were then spin coated with AZ1518 photoresist. Arrays of 300 μm diameter circular Schottky contacts were patterned by UV lithography and developed using tetramethyl ammomium hydroxide (TMAH) for 20 s followed by a final rinse in de-ionized (DI) H_2O and drying in N_2. A 40 nm thick silver oxide film was then deposited by the reactive rf sputtering of a Ag target (99.99% purity) using an Ar/O_2 plasma, a rf power of 50 W, and a processing pressure of 4×10^{-3} mbar. A Pt capping layer was then deposited onto the silver oxide film by e-beam evaporation. Following the lift-off of the silver oxide/Pt bilayer, annular Ti/Al/Pt Ohmic rings were fabricated using lift-off photolithography and e-beam evaporation. The annular gap between the Schottky and Ohmic contacts was 25 μm.

In order to investigate the condition of the ZnO surface prior to silver oxide deposition, variable angle, x-ray photoelectron spectroscopy (XPS) was performed on the Zn-polar and O-polar faces of a hydrothermal ZnO wafer immediately after developing with TMAH/DI H_2O/N_2. Figure 2 shows

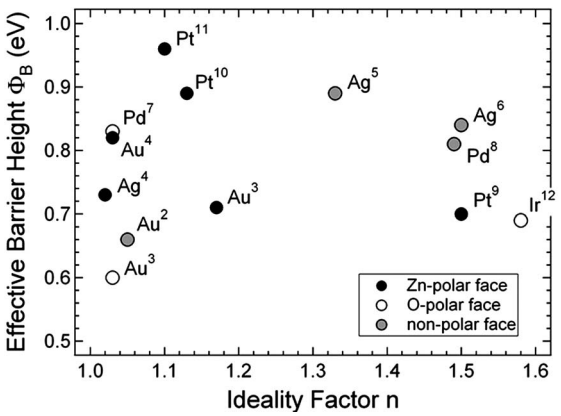

FIG. 1. Effective barrier height (Φ_B) vs ideality factor (n) for the best reported Schottky contacts on *n*-type ZnO.

[a]Electronic mail: martin.allen@elec.canterbury.ac.nz

TABLE I. Electrical characterization of hydrothermal and melt grown ZnO wafers from single field (0.51 T) Hall effect measurements at RT [carrier concentration ($N_{D,\mathrm{Hall}}$), mobility (μ), and resistivity (ρ)].

Wafer	$(N_{D,\mathrm{Hall}})$ (cm^{-3})	μ $(\mathrm{cm}^2\,\mathrm{V}^{-1}\,\mathrm{s}^{-1})$	ρ $(\Omega\,\mathrm{cm})$
HT-1	1.2×10^{14}	190	300
PM-1 Zn polar	1.1×10^{17}	184	0.30
PM-2 O polar	7.4×10^{16}	187	0.45
PM-3 *a* plane	5.3×10^{16}	187	0.63

the O 1s core level spectra. Two main oxygen species can be identified: a peak at 531.0 eV due to ZnO lattice oxygen and a peak at 532.8 eV due to hydroxyl groups. The spectra remained unchanged after a further 24 h in vacuum conditions ($\sim5\times10^{-8}$ m bar), indicating both faces contained a uniform layer of hydroxide (estimated thickness ~0.6 nm using the method of Spruytte *et al.*[17]) prior to Schottky contact deposition.

The silver oxide Schottky diodes were characterized by current-voltage (*I-V*) and capacitance-voltage (*C-V*) measurements at room temperature, in dark conditions, and with the diodes exposed to air. Figures 3(a) and 3(b) show the *I-V* characteristics of the best silver oxide diodes. The diodes on both types of bulk ZnO have very high rectifying ratios, in excess of 10^8V at ±1 V. The diodes on hydrothermal ZnO have a smaller reverse current voltage dependence while those on melt ZnO have a lower series resistance R_s. The current transport through a Schottky junction can be described by the thermionic emission (TE) of majority carriers over the junction barrier using

$$J = A^{*}T^{2}\exp\left(\frac{-q\Phi_B}{kT}\right)\left\{\exp\left[\frac{(qV-JR_s)}{nkT}\right]-1\right\}, \qquad (1)$$

where A^* is the effective Richardson constant, which for ZnO has a theoretical value of 32 A cm^{-2} K^{-2}. Equation (1) was used to determine Φ_B and n for a number of silver oxide diodes on each sample and these are plotted against each other in Figs. 3(c) and 3(d). These plots confirm the previously reported polarity effect for hydrothermal ZnO,[18] with diodes on the Zn-polar face having approximately 200 meV higher barriers than those on the O-polar face. A much smaller polarity effect is evident for diodes on melt ZnO, with a barrier height difference of only 50 meV between the Zn-polar and O-polar faces. Diodes on the nonpolar, *a*-plane face have intermediate barrier heights, which is similar to the case for *m*-plane diodes on hydrothermal ZnO.[4]

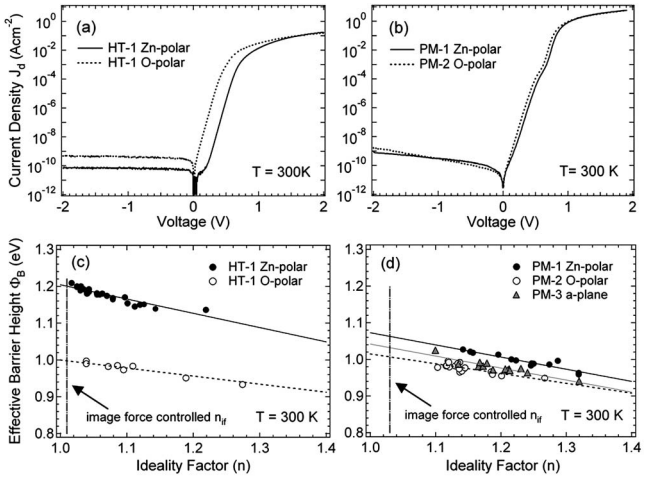

FIG. 3. Typical *I-V* characteristics and effective barrier height (Φ_B) vs ideality factor (n) plots, measured at RT, for silver oxide diodes on hydrothermal and melt bulk ZnO.

Figures 4(a) and 4(b) show the *C-V* characteristics of the best silver oxide contacts. The capacitance of a Schottky junction is given by

$$\frac{A^2}{C^2} = \left(\frac{2}{\varepsilon_s\varepsilon_0 N_D}\right)\left(V_{\mathrm{bi}} - \frac{kT}{q} - V\right), \qquad (2)$$

where A is the junction area, ε_s is the static dielectric constant, and V_{bi} is the built-in potential. Table II gives the values of Φ_B from *C-V* measurements: $\Phi_{B,C\text{-}V}=V_{\mathrm{bi}}+\xi$, where $\xi=kT/q\,\ln(N_C/N_D)$ is the energy difference between the Fermi level and the bottom of the conduction band (N_C is the conduction band density of states $= 2.94\times10^{18}$ cm^{-3}). Figures 4(c) and 4(d) show the effective donor concentration depth profile for each sample, using Eq. (2) and $C=\varepsilon_s\varepsilon_0 A/\mathrm{d}$, where d is the depletion region width. These profiles show a lower donor concentration near the Zn-polar face compared to the O-polar face.

For each of the Φ_B vs n plots in Fig. 3, Φ_B becomes smaller with increasing n. This is due to increasing lateral inhomogeneity of the Schottky contacts.[19] The real barrier

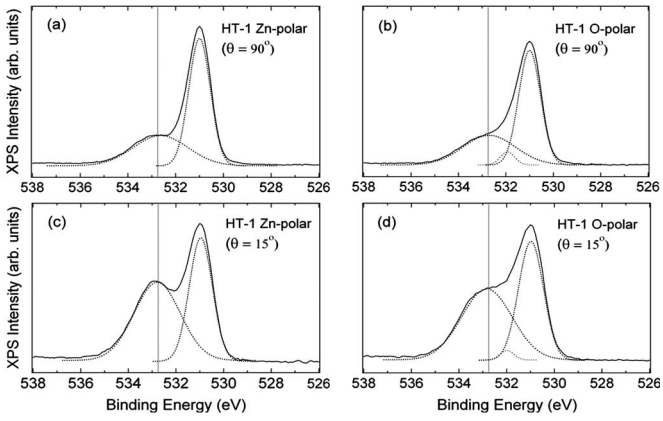

FIG. 2. Variable angle XPS of the O 1s core level on the Zn-polar and O-polar faces of hydrothermal bulk ZnO, for takeoff angles of 90° and 15°, after TMAH treatment (20 s), DI H_2O rinsing, and drying with N_2.

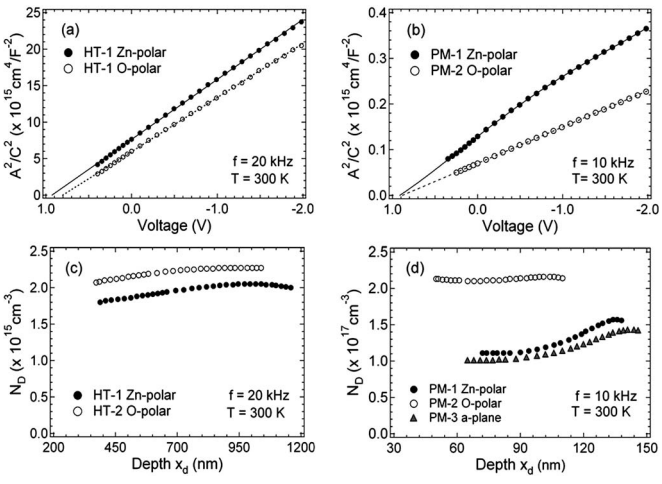

FIG. 4. Typical *C-V* characteristics and effective donor concentration depth profiles, measured at RT, for silver oxide diodes on hydrothermal and melt bulk ZnO.

TABLE II. Characteristics of the best silver oxide diodes on hydrothermal and melt bulk ZnO wafers from *I-V* and *C-V* measurements at RT, and calculated image force lowering and tunneling parameters [ideality factor (n), barrier height ($\Phi_{B,I\text{-}V}$), built in potential ($\Phi_{\mathrm{bi},C\text{-}V}$), barrier height ($\Phi_{B,C\text{-}V}$), effective donor density ($N_{D,C\text{-}V}$), image force lowering of Φ_B ($\Delta\Phi_{\mathrm{if}}$), image force controlled ideality factor (n_{if}), laterally homogeneous barrier height (Φ_B^{hom}), tunneling parameter (E_{00}/kT), and TFE controlled ideality factor (n_{tun})].

Sample	n	$\Phi_{B,I\text{-}V}$ (eV)	$\Phi_{\mathrm{bi},C\text{-}V}$ (eV)	$\Phi_{B,C\text{-}V}$ (eV)	$N_{D,C\text{-}V}$ (cm^{-3})	$\Delta\Phi_{\mathrm{if}}$ (eV)	n_{if}	Φ_B^{hom} (eV)	E_{00}/kT (at 300 K)	n_{tun}
HT-1 Zn polar	1.03	1.20	0.93	1.20	2.0×10^{15}	0.03	1.01	1.20	0.005	1.000
HT-1 O polar	1.04	0.99	0.79	1.06	2.2×10^{15}	0.03	1.01	1.00	0.005	1.000
PM-1 Zn polar	1.14	1.03	⋯	⋯	1.5×10^{17}	0.10	1.03	1.06	0.16	1.008
PM-2 O polar	1.10	0.98	0.89	1.04	2.1×10^{17}	0.10	1.03	1.01	0.13	1.006
PM-3 *A* plane	1.10	1.02	⋯	⋯	1.4×10^{15}	0.10	1.03	1.03	0.11	1.004

height of laterally homogeneous contacts Φ_B^{hom}, can be obtained by the extrapolation of these plots to the corresponding image force controlled ideality factor n_{if},[19]

$$\frac{1}{n_{\mathrm{if}}} = 1 - \frac{\Delta\Phi_{\mathrm{if}}}{4}\left(\Phi_B - V - \xi - \frac{kT}{q}\right)^{-1}, \tag{3}$$

$$\Delta\Phi_{\mathrm{if}} = \left[\left(\frac{q^3 N_D}{8\pi^2\varepsilon_\infty^2\varepsilon_s\varepsilon_0^3}\right)\left(\Phi_B - V - \xi - \frac{kT}{q}\right)\right]^{1/4}, \tag{4}$$

where $\Delta\Phi_{\mathrm{if}}$ is the image force lowering of the barrier height, V is the bias voltage, and ε_∞ is the optical dielectric constant. Table II gives the zero bias values of $\Delta\Phi_{\mathrm{if}}$ and n_{if} (using N_D from *C-V* measurements), and Φ_B^{hom} extrapolated from Figs. 3(c) and 3(d). The influence of image force lowering is greater for the diodes on melt ZnO, but for neither material does image force lowering fully explain the measured ideality factors of the best diodes.

Another possible contributor to nonideal behavior is thermionic field emission (TFE). The parameter E_{00} determines the relative importance of tunneling to TE,[20]

$$E_{00} = \frac{qh}{4\pi}\left(\frac{N_D}{m^*\varepsilon_s\varepsilon_0}\right)^{1/2}, \tag{5}$$

where m^* is the electron effective mass. TFE becomes significant when $E_{00}\sim kT$. E_{00} can also be used to determine the ideality factor n_{tun} due to TFE.[13] Table II shows the values of E_{00}/kT and n_{tun} for each sample. Here $N_{D,\mathrm{Hall}}$ (Table I) was used, as E_{00} is a bulk property. These parameters indicate that TFE is insignificant for silver oxide diodes on hydrothermal ZnO and causes only a small increase in ideality factor for diodes on melt ZnO. However, the presence of traps in the depletion region can increase the tunneling probability, and consequently, n_{tun} as carriers can first tunnel into these traps and then through the barrier.

In summary, highly rectifying silver oxide Schottky contacts were fabricated on hydrothermal and melt grown, bulk ZnO wafers whose resistivities differ by nearly three orders of magnitude. A polarity effect was observed on both types of bulk ZnO in that silver oxide diodes fabricated on the Zn-polar face had higher barriers than those on the O-polar face. This effect was much larger on the high resistivity hydrothermal ZnO. This is consistent with a previously described model of surface band bending, due to the large spontaneous polarization of ZnO along the c axis,[18] in which the upward band bending at the Zn-polar face increases with decreasing carrier concentration. The silver oxide contacts on melt ZnO had higher ideality factors and a larger reverse current voltage dependence. This again is largely due to the higher carrier concentration of melt ZnO which makes image force lowering and thermionic field emission effects more significant. Variable angle XPS showed that both the Zn-polar and O-polar ZnO surfaces are covered with an ~0.6 nm thick hydroxide layer prior to Schottky contact deposition. It is possible that the oxygen plasma used in the fabrication of the silver oxide contacts has the beneficial effect of removing this contamination. However, the best reported Au and Pt Schottky contacts[4,11] have been achieved on hydrothermal bulk ZnO with an identical sample preparation to the one used here but without any plasma being involved.

The authors acknowledge the help of C. Doyle, B. James, P. Miller, and R. J. Reeves. This work was supported by the Marsden Fund (06UOC022) and The MacDiarmid Institute for Advanced Materials and Nanotechnology.

[1] D. C. Look, J. Electron. Mater. **35**, 1299 (2006).
[2] C. A. Mead, Phys. Lett. **18**, 218 (1965).
[3] B. J. Coppa, C. C. Fulton, S. M. Kiesel, R. F. Davis, C. Pandarinath, J. E. Burnette, R. J. Nemanich, and D. J. Smith, J. Appl. Phys. **97**, 103517 (2005).
[4] M. W. Allen, P. Miller, J. B. Metson, R. J. Reeves, M. M. Alkaisi, and S. M. Durbin, Mater. Res. Soc. Symp. Proc. **0957**, K09–03 (2006).
[5] H. Sheng, S. Muthukumar, N. W. Emanetoglu, and Y. Lu, Appl. Phys. Lett. **80**, 2132 (2002).
[6] S. Liang, H. Sheng, Y. Lui, Z. Huo, Y. Lu, and H. Shen, J. Cryst. Growth **225**, 110 (2000).
[7] U. Grossner, S. Gabrielsen, T. M. Borseth, J. Grillenberger, A. Y. Kuznetsov, and B. G. Svensson, Appl. Phys. Lett. **85**, 2259 (2004).
[8] H. von Wenckstern, G. Biehne, R. A. Rahman, H. Hochmuth, M. Lorenz, and M. Grundmann, Appl. Phys. Lett. **88**, 092102 (2006).
[9] K. Ip, B. P. Gila, A. H. Onstine, E. S. Lambers, Y. W. Heo, K. H. Baik, D. P. Norton, S. J. Pearton, S. Kim, J. R. LaRoche, and F. Ren, Appl. Surf. Sci. **236**, 387 (2004).
[10] S. H. Kim, H. K. Kim, and T. Y. Seong, Appl. Phys. Lett. **86**, 112101 (2005).
[11] H. Endo, M. Sugibuchi, K. Takahashi, S. Goto, S. Sugimura, K. Hane, and Y. Kashiwaba, Appl. Phys. Lett. **90**, 121906 (2007).
[12] L. J. Brillson, H. L. Mosbacker, M. J. Hetzer, Y. Strzhemechny, G. H. Jessen, D. C. Look, G. Cantwell, J. Zhang, and J. J. Song, Appl. Phys. Lett. **90**, 102116 (2007).
[13] R. T. Tung, Mater. Sci. Eng., R. **35**, 1 (2001).
[14] V. A. Coleman, Ph.D. thesis, Australian National University, 2006.
[15] K. Maeda, M. Sato, I. Niikura, and T. Fukuda, Semicond. Sci. Technol. **20**, S49 (2005).
[16] J. Nause and B. Nemeth, Semicond. Sci. Technol. **20**, S45 (2005).
[17] S. Spruytte, C. Coldren, J. Harris, D. Pantelidis, H. J. Lee, J. Bravman, and M. Kelly, J. Vac. Sci. Technol. A **19**, 603 (2001).
[18] M. W. Allen, P. Miller, R. J. Reeves, and S. M. Durbin, Appl. Phys. Lett. **90**, 062104 (2007).
[19] W. Mönch, J. Vac. Sci. Technol. B **17**, 1867 (1999).
[20] F. A. Padovani and R. Stratton, Solid-State Electron. **9**, 695 (1966).